Optical Detection of Attosecond Ionization Induced by a Few-Cycle Laser Field in a Transparent Dielectric Material

Alexander V. Mitrofanov,[1] Aart J. Verhoef,[1] Evgenii E. Serebryannikov,[2] Julien Lumeau,[3] Leonid Glebov,[3] Aleksei M. Zheltikov,[2] and Andrius Baltuška[1]

[1]*Photonics Institute, Vienna University of Technology, Gusshausstrasse 27-29/387, A-1040, Vienna, Austria*
[2]*Physics Department, International Laser Center, M.V. Lomonosov Moscow State University, Vorobyevy gory, 119992 Moscow, Russia*
[3]*CREOL, University of Central Florida, Orlando, Florida 32816, USA*

(Received 18 November 2010; published 4 April 2011)

We observe an optical signature induced by the modulation of electron density inside a bulk transparent solid that is quasiperiodically ionized on an attosecond time scale by electric field peaks of a focused few-cycle laser pulse. The emitted optical signal resulting from the attosecond ionization dynamics is spatially, temporally and spectrally isolated from concomitant optical responses through the use of a noncollinear pump-probe technique. The method holds promise for developing an attosecond metrology for bulk solids, in which, unlike in the established attosecond metrology of gases and surfaces, direct detection of charged particles is unfeasible.

DOI: 10.1103/PhysRevLett.106.147401 PACS numbers: 78.20.-e, 42.90.+m, 78.47.J−

The interaction of intense laser pulses with dielectric materials recently became an object of great interest both from the viewpoint of fundamental physics and applications. The complex interaction dynamics begins with the generation of free carriers via different mechanisms of ionization that depend on various material properties and characteristics of the laser pulse, such as the structure and the size of the dielectric band gap, the carrier frequency and the peak instantaneous amplitude of the laser field, its polarization, and the laser pulse duration. Ionization of solids in a laser field holds the key to many applications including the writing of waveguides in a bulk solid and material ablation by ultrashort laser pulses [1]. In optical breakdown of dielectrics, the optical field ionization precedes the development of avalanche ionization and, therefore, acts as an initial step in the formation of an optical damage by a femtosecond pulse [2]. Whereas such irreversible changes have been extensively studied, the mapping of subcycle ionization dynamics in solids is an open challenge.

Ionization in dielectrics is understood as an electron transition from the valence into the conduction band. The presence of interband transitions and heavy collisional dynamics complicate the process of free-electron plasma buildup in a dielectric in comparison with the more straightforward case of ionization of atoms and molecules, where the electrons are transferred from a bound state into a continuum. When the photon energy of the laser light is less than the band gap of a solid or the binding potential of an atom, the energy of many photons has to be supplied simultaneously to promote an electron into the conduction band-continuum, resulting in a strong dependence of the ionization rate on the laser intensity. In addition, in the strong-field regime, the ionization rate becomes dependent not just on the intensity envelope but also on the instantaneous field strength of the pulse, because the binding potential of the weakest bound electrons is strongly suppressed near the peaks of intense half-cycles of the electric field of a linearly polarized laser pulse, as schematically depicted in Fig. 1, right. In this regime, one expects attosecond ionization bursts to occur in the vicinity of field peaks with a twice-per-cycle periodicity (Fig. 1, left) [3–5]. The stepwise plasma density increase in gas was confirmed experimentally in a direct attosecond measurement [6].

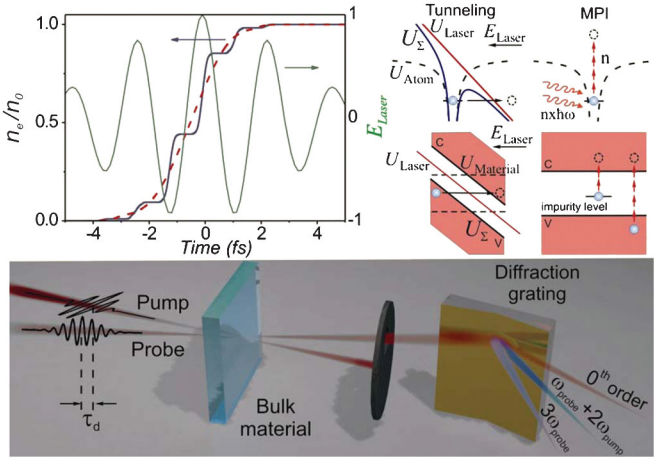

FIG. 1 (color). A weak probe pulse reads out the pump-induced electron density modulation in the form of new spectral components propagating along its direction ($\omega_{probe} + 2\omega_{pump}$). Left top: The pump field $E(t)$ (green line) and temporal profiles of the electron density calculated with the use of the standard Keldysh-type model with a cycle-averaged field intensity (red dashed line) and the modified Keldysh model with an instantaneous field intensity (blue solid line). The intensity used here is 2×10^{13} W/cm^2. Right top: different regimes of ionization: tunneling (on the left) and multiphoton (on the right).

In an analogy with atomic ionization, a similar stepwise population increase in the conduction band can be expected in a bulk medium ionized with a few-cycle pulse. However, the established metrology for studying attosecond dynamics [7] in gas [6] and on solid surfaces [8] is inapplicable for solid bulk targets. Seeking an alternative based on all-optical detection, Gerstvolf *et al.* have linked the subcycle formation of free carriers to nonlinear absorption and ellipticity change of an ionizing optical pulse transmitted through bulk silica and pointed out that, with the increase of pulse duration, the effect of subcycle ionization on femtosecond ellipsometry data is masked by collisional dynamics [9]. In this Letter we present strong evidence for subcycle free carrier formation in several transparent dielectrics which is visualized by the emission of a background-free optical signal that can be unequivocally decoupled from other nonlinear processes in a transparent bulk dielectric. The observed optical signal originated from a frequency transformation of a weak probe pulse traveling through a bulk volume where the free-electron density changes in sharp attosecond steps as a result of interaction with an intense few-cycle ionizing pulse.

The experimental approach exploited in this work is based on the noncollinear two-color pump-probe arrangement which is schematically shown on Fig. 1. An ultrashort linearly polarized pulse with central wavelength around 750 nm is split in two: one temporally compressed few-cycle (~ 5 fs) pump pulse with energy up to 10 μJ and a weak cross-polarized probe pulse which additionally propagates through an interference filter. After the filter it has a central wavelength of 850 nm and a duration of $\sim$40 fs. Both pump and probe pulses are focused into the media under investigation in a noncollinear manner crossing under an angle of 1.5°. The pump pulse intensity can be varied with an adjustable iris and can reach 30 TW/cm^2 under our focusing conditions. Using this method, we have investigated ionization dynamics in bulk transparent dielectrics with different band gaps.

A quasiperiodic subcycle modulation leads to the generation of sidebands at frequencies $\omega_{\text{probe}} + n \times 2\omega_{\text{pump}}$, where n-integer number. The use of a noncollinear geometry, cross-polarized pump and probe beams [10], and nondegenerate frequencies permits the suppression of concomitant signals which includes third harmonic generation of the pump and probe beams and four-wave mixing signals ($\omega_{\text{pump}} + 2\omega_{\text{probe}}$ and $2\omega_{\text{pump}} + \omega_{\text{probe}}$).

Thereby, with the above described experimental setup we were able to detect the optical signal at a new frequency that, to our belief, is proof of ionization dynamics, sensitive directly to the optical field of the ionizing pulse and going on subcycle time scale. The regarded technique can be considered as a promising tool for investigation of subcycle ionization dynamics in bulk transparent media. However, quantitative retrieval of these dynamics requires the detection of ionization induced sidebands of several higher orders. A possible way to go would be to use OPA systems delivering few-cycle pulses in the near- and mid-IR spectral range [11], which allows staying in the transparency range even for second- and third-order ionization induced sidebands. In addition to that, propagation effects play a non-negligible role, influencing both the pump and the probe pulses and will make the retrieval more complicated. However, as it was demonstrated by calculations in Refs. [10,12] the effective interaction volume responsible for the emission of the optical ionization signature is able to self-adjust with respect to the incoming pump pulse intensity, leading to the same yield of the ionization induced sideband.

We have detected the first ionization induced sideband using a 0.5 mm thick fused silica plate as a test sample and investigated its dependence on the polarization state of the pump pulse (Fig. 2). The pump intensity was adjusted to be below the level of optical damage ($< 2 \times 10^{13}$ W/cm^2). To confirm the origin of the observed signal, the experiments were repeated with linear and circularly polarized pump fields.

For linearly polarized pump pulses we were able to reliably detect the ionization induced sideband at a wavelength around 260 nm [Fig. 2(a)], exactly where it is expected according to the theoretical prediction, spectrally separated from the direct third harmonic of the probe beam, which is expected and observed at 285 nm. The ionization induced signal is strongly delay-dependent and follows the probe envelope since it is generated only when

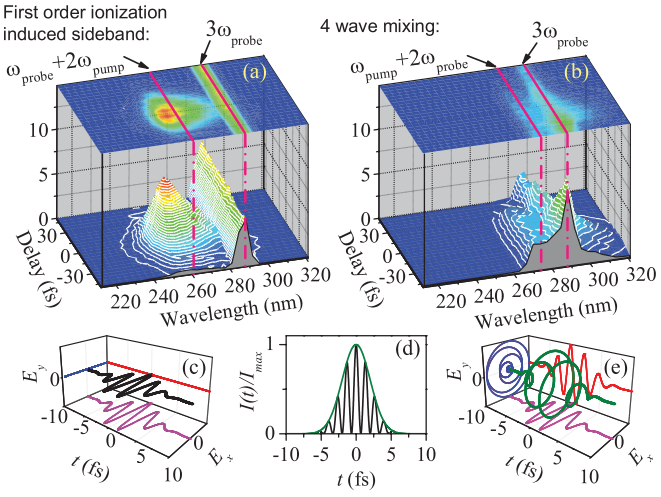

FIG. 2 (color). Measurement of the first ionization induced sideband for linear (a) and circular (b) pump polarizations in a 0.5 mm thick fused silica plate. (c) and (e) represent the polarization state of the pump pulse for, respectively, (a) and (b). The electric field is shown in black (linear polarization) and green (circular polarization). Panel (d) shows the instantaneous intensity of the field for linear polarization (black line) and circular polarization (green line).

the probe pulse sees the subcycle temporal modulation of the free-electron density caused by the pump pulse (see Fig. 1, left panel), while the third harmonic of the probe is delay independent [Fig. 2(a)]. For circular polarization of the pump pulses, no signal was observed in this spectral range up to the threshold for optical damage, except for a weak delay-dependent signal at around 270 nm [Fig. 2(b)], which we attribute to the four-wave mixing process at frequency $\omega_{\text{pump}} + 2\omega_{\text{probe}}$ due to the $\chi^{\langle 3\rangle}$ nonlinearity of the glass. Note that this signal inherits its polarization from the pump pulses; thus, for circularly polarized pump pulses it can leak through the polarizer whereas it is blocked in the case of linear polarization. The disappearance of the frequency sideband $\omega_{\text{probe}} + 2\omega_{\text{pump}}$ collinear with the probe beam direction in the case of a circularly polarized pump is explained by the absence of quasiperiodic peaks of the ionization yield.

The experimentally measured time-frequency map shown in Fig. 2(a) was analyzed using a full 3D few-cycle pulse propagation model in an ionizing solid dielectric. This model is based on the numerical solution of the generalized nonlinear Schrödinger equation (GNSE) including dispersion and diffraction effects, plasma absorption and refraction, electronic (Kerr) and retarded (Raman) optical nonlinearities, as well as nonlinearities induced by ionization effects (see [13,14] for the details of the model). The GNSE is solved jointly with the equation for the electron-density dynamics including photoionization and impact ionization. Calculation of the field-phase-sensitive photoionization rate in solids encounters difficulties as the Keldysh-type formulas [15] operate with a field intensity averaged over the field cycle, while closedform solutions, similar to the Yudin—Ivanov formula [5] for photoionization in gases, are lacking. In view of this difficulty, we calculate the photoionization rate using a generic ansatz based on the Keldysh formalism with the cycle-averaged field intensity replaced by the instantaneous field intensity. Temporal profiles of the electron density n_e calculated with the use of this approach (solid blue line in the left panel of Fig. 1) display well-resolved steps locked to field half-cycles [12]. With an appropriate choice of a single normalization constant in front of the tunneling exponential, the electron density generated by the end of the laser pulse in our model (instants of time exceeding 3 fs in the left panel of Fig. 1) deviates by less than 0.5% from the prediction of the standard Keldysh-type model with a cycle-averaged field intensity (cf. the solid blue and dashed red lines in the left panel of Fig. 1). The impact ionization is simulated using a Drude-type model [13,14] for the inverse bremsstrahlung cross section with an electron collision time of 10 fs.

The spectrogram of the first ionization induced sideband calculated using this model under the conditions of our experiment is shown in Fig. 3(a), revealing good agreement with the experimental map [Fig. 3(b)]. Spectra at zero delay for both the theoretical calculations and the experiment are shown in Fig. 3(c). A rapid drop of the experimentally measured signal at shorter wavelengths is dictated by the transparency range of the polarizer which was used before the detector. The pump pulse at the output of the fused silica plate is spectrally broadened due to self-phase modulation and rapid ionization [Fig. 3(d)].

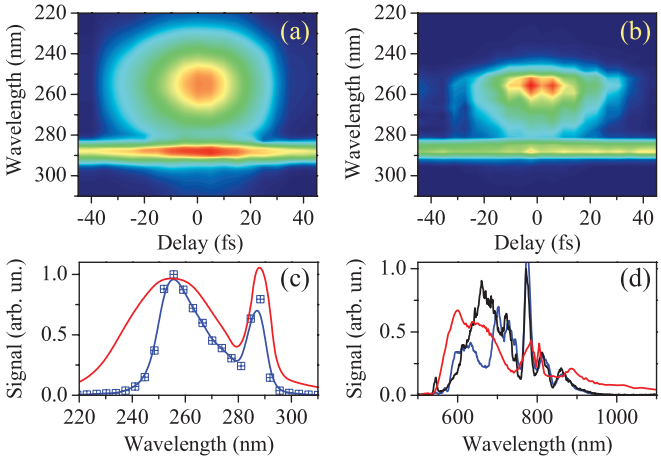

FIG. 3 (color). Simulated (a) and experimentally measured (b) spectrograms obtained from a 0.5 mm thick fused silica plate. (c) Spectra at zero delay (red—simulated, blue—experimental). (d) Initial spectrum (black curve) of the pump pulse and transmitted spectra after propagation through the plate (red—calculated, blue—experimentally).

Since the ionization process is very sensitive to the amplitude of the ionizing field, the ionization induced sideband is expected to be strongly dependent on the intensity of the pump pulse. The spectra at zero delay of the ionization induced sideband together with the third

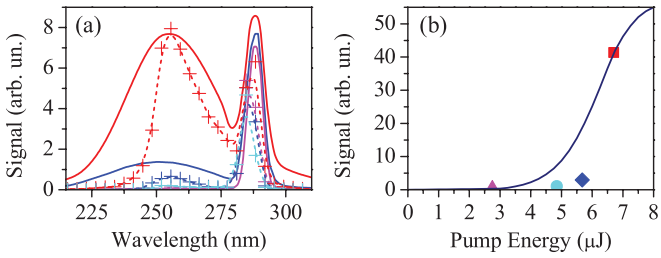

FIG. 4 (color). (a) Spectra of the ionization induced sideband and direct third harmonic of the probe (at zero delay) for different pump pulse energies. Simulated spectra are shown by solid lines for 6.7 μJ (red line), 5 μJ (blue) and 3 μJ (magenta) pump pulse energy. The experimentally measured spectra are depicted by crosses connected with dashed lines for ~6.7 μJ (red), ~5.6 μJ (blue), ~4.5 μJ (cyan) and ~3 μJ (magenta). (b) Spectrally integrated energy (from 220 nm to 277 nm) of the ionization induced sideband versus pump pulse energy. Solid line—simulated data, separate dots—experimental data. The absolute experimental value at the highest pump energy is put equal to the value obtained in the calculations, and the other experimental points are scaled accordingly.

TABLE I. Amplitude of the ionization induced signal for different materials with known band gap. $\chi^{\langle 3\rangle}$ signal—is the amplitude of direct third harmonic of the probe pulse. SLS (soda lime silicate) is $Na_2O(22\%)CaO(3\%)SiO_2(75\%)$. Note that the crystalline CaF_2 is a centrosymmetric crystal, and in MgF_2 the light propagation was along the principle axis.

Material	Band gap (eV)	Sig. amplitude (arb.un.)	$\chi^{\langle 3\rangle}$ signal (arb.un.)
SLS	6.5	83	20
Fused silica	9	794	640
CaF_2	10	285	30
MgF_2	11	33	230

harmonic of the probe beam, for different pump pulse intensities, are shown in Fig. 4(a). The amplitude of the ionization induced sideband rapidly grows with pump pulse intensity [see Fig. 4(b)] as expected from exponential dependence of the ionization yield. The experimental curve shows, however, a much faster rise in comparison to the simulations. A possible explanation to that can be the fact that the size of the band gap of the sample is not precisely known, while it can greatly affect the ionization rate.

To determine the influence of the band structure on the ionization dynamics we performed similar measurements in several different solid transparent dielectrics with known band gaps. Since for a fixed field strength the ionization rate depends critically on the ionization potential, or band gap, the ionization induced sideband is expected to be different in materials with different band gaps. In addition to the size of the band gap, the presence of impurities in the sample under investigation may play a significant role in suppressing or promoting ionization in the laser field. For example, samples with impurities are known to be more prone to optical damage than very pure samples of the same material. For crystalline materials the orientation of the crystal axes with respect to the laser polarization can influence ionization as well [16]. For several materials the maximum ionization induced signal is summarized in Table I. The pump pulse energy was set to $\sim 6.7\ \mu$J in all cases. As it can be seen from the table, the general tendency is that for materials with a larger band gap the ionization induced signal drops dramatically. The exception to this rule was only soda lime silicate which has the smallest band gap, however which did not exhibit a very strong ionization induced response. The nonlinear $\chi^{\langle 3\rangle}$ response of this material was also very low.

In conclusion, we demonstrated a new method enabling the detection of subcycle ionization dynamics in bulk transparent media based on optical harmonic generation due to an ultrafast modulation of free-electron density during ionization. The noncollinear frequency- and time-resolved pump-probe technique allows us to isolate the ionization induced optical signal both spectrally and spatially from optical signals originating from other nonlinearities of the medium. We have demonstrated a strong dependence of the ionization induced signal on the intensity of the pump pulse and also on the size of the material band gap. Our technique represents an alternative approach to the methods of attosecond metrology based on detection of particles or high harmonic spectroscopy, allowing an extension of spectroscopic and imaging technologies capable of analyzing attosecond electron dynamics in large molecules and bulk solids.

This research has been supported by the Austrian Science Fund (Grants No. U33-N16 and No. I185-N14), EU FP7 (CROSSTRAP, Grant No. 244068), EUROSTARS (YAFFLE, Grant No. 4319), the Russian Federal Science and Technology Program (Contracts No. 1130 and No. 02.740.11.0223) and the Russian Foundation for Basic Research (Project No. 09-02-91004, No. 09-02-12359, and No. 09-02-12373).

[1] Rafael R. Gattass and Eric Mazur, Nat. Photon. **2**, 219 (2008).
[2] M. Lenzner *et al.*, Phys. Rev. Lett. **80**, 4076 (1998).
[3] F. Brunel, J. Opt. Soc. Am. B **7**, 521 (1990).
[4] C. Siders *et al.*, Phys. Rev. Lett. **87**, 263002 (2001)
[5] G. Yudin and M. Ivanov, Phys. Rev. A **64**, 013409 (2001).
[6] M. Uiberacker *et al.*, Nature (London) **446**, 627 (2007).
[7] F. Krausz and M. Ivanov, Rev. Mod. Phys. **81**, 163 (2009).
[8] A. Cavalieri *et al.*, Nature (London) **449**, 1029 (2007).
[9] M. Gertsvolf *et al.*, J. Phys. B **43**, 131002 (2010).
[10] A. Verhoef *et al.*, Phys. Rev. Lett. **104**, 163904 (2010).
[11] O. D. Mücke *et al.*, Opt. Lett. **34**, 2498 (2009).
[12] E. Serebryannikov *et al.*, Phys. Rev. A **80**, 053809 (2009).
[13] L. Bergé *et al.*, Rep. Prog. Phys. **70**, 1633 (2007).
[14] A. Couairon and A. Mysyrowicz, Phys. Rep. **441**, 47 (2007).
[15] L. V. Keldysh, Sov. Phys. JETP **20**, 1307 (1965).
[16] Gerstvolf *et al.*, Phys. Rev. Lett. **101**, 243001 (2008).